Analytical and numerical stability analysis of Soret-driven convection in a horizontal porous layer: The effect of vertical vibrations

Soumaya Ouadhani, Ali Abdenadher, Abdelkader Mojtabi

Analytical and numerical stability analysis of Soret-driven convection in a horizontal porous layer: The effect of vertical vibrations*

Soumaya Ouadhani[1,2], Ali Abdennadher[2], and Abdelkader Mojtabi[1,a]

[1] IMFT, UMR CNRS/INP/UPS No. 5502, UFR MIG, Paul Sabatier University, 118 Narbonne street, 31062 Toulouse cedex, France
[2] Carthage University, LIM Laboratory, Polytechnic School of Tunisia, BP 743, 2078 Marsa, Tunisia

Abstract. The authors studied the effect of vertical high-frequency and small-amplitude vibrations on the separation of a binary mixture saturating a porous cavity. The horizontal bottom plate was submitted to constant uniform heat flux and the top one was maintained at constant temperature while no mass flux was imposed. The influence of vertical vibrations on the onset of convection and on the stability of the unicellular flow was investigated for positive separation ratio ψ. The case of high-frequency and small-amplitude vibrations was considered so that a formulation using time averaged equations could be used. For an infinite horizontal porous layer, the equilibrium solution was found to lose its stability via a stationary bifurcation leading to unicellular flow or multicellular one depending on the value of ψ. The analytical solution of the unicellular flow was obtained and separation was expressed in terms of Lewis number, separation ratio and thermal Rayleigh number. The direct numerical simulations using the averaged governing equations and analytical stability analysis showed that the unicellular flow loses its stability via oscillatory bifurcation. The vibrations decrease the value of ψ_{uni}, which allows species separation for a wide variety of binary mixtures. The vibrations can be used to maintain the unicellular flow and allow species separation over a wider range of Rayleigh numbers. The results of direct numerical simulations and analytical model are in good agreement.

1 Introduction

Double-diffusive convection caused by temperature and concentration gradients in a porous medium is a classical example of the problems that reveal the interaction of different instability mechanisms. Reviews of recent developments and publications in this field can be found in [1]. A great number of works in this field of research are devoted to investigation into high-frequency and small amplitude vibration. Khallouf *et al.* [2] considered a square differentially heated cavity filled with a porous medium saturated by a pure fluid and subjected to linear harmonic oscillations in the vertical direction. In their study, the authors used a Darcy-Boussinesq model and a direct formulation. Gershuni *et al.* [3] have studied the stability of a substantially linear mechanical equilibrium solution for an horizontal layer of a binary mixture subjected to vertical thermal gradient under the effect of high-frequency vibrations. The thermovibrational convection in a fluid received more attention than the thermovibrational convection in a porous medium. A good summary of this work was achieved by Gershuni *et al.* [4, 5].

In the case of a horizontal porous layer saturated by a pure fluid, heated from below or from above Zenkovskaya *et al.* [6] and Bardan *et al.* [7] used the Darcy model including the non-stationary term and adopted the time-averaged equations formulation to study the influence of high-frequency and small-amplitude vibrations on the onset of convection. They found that vertical vibrations stabilize the rest solution. Charrier-Mojtabi *et al.* [8] investigated the influence of vibrations on Soret-driven convection in a horizontal porous cell heated from below or from above. They showed that the vertical vibrations had a stabilizing effect while the horizontal vibrations had a destabilizing effect. Elhajjar *et al.* [9] have studied the influence of the vertical vibration of high frequency and small amplitude on separation for a cell with horizontal walls maintained at constant but different temperatures. The linear stability of the unicellular flow obtained was analyzed analytically and numerically. They concluded

* Contribution to the Topical Issue "Non-isothermal transport in complex fluids", edited by Rafael Delgado-Buscalioni, Mohamed Khayet, José María Ortiz de Zárate and Fabrizio Croccolo.

[a] e-mail: mojtabi@imft.fr

that the unicellular flow associated with a field of laminate concentration leads to the horizontal separation of binary mixture components. They found that the vibrations have a stabilizing effect, leading to an increase of the critical value of the Rayleigh number corresponding to the transition between the unicellular and multicellular flow. Consequently vertical vibration allows species separation for a wide variety of binary mixtures. The validity of the average approach for the description of vibrational convection in porous medium differs from the case with homogeneous fluid and is not widely known. This point is developed in more details in the paper by Lyubimov *et al.* [10]. The authors investigated the onset and nonlinear regimes of convection in a two-layer system composed of a horizontal pure fluid layer and a fluid-saturated porous layer subjected to the gravity field and high-frequency vibrations.

In the present paper, we use the same formulation as the one used by Charrier-Mojtabi *et al.* [8] for a shallow porous cavity saturated by a binary mixture. The cavity bounded by horizontal infinite or finite boundaries. The bottom horizontal plate is submitted to constant uniform heat flux and the top one is maintained at constant temperature, while no mass flux is imposed. We verify that it is possible to carry out the species separation of a binary mixture in this geometrical configuration. We consider the case of high-frequency and small-amplitude vibrations, so that a formulation using time averaged equations can be employed. The results of the linear stability analysis of the mechanical equilibrium and the unicellular flow in an infinite porous layer is studied analytically and using spectral method.

2 Mathematical formulation

We consider a rectangular cavity with aspect ratio $A = L/H$, where H is the height of the cavity along the vertical axis and L is the width along the horizontal axis (fig. 1). The aspect ratio is assumed infinite in the stability analysis. The cavity is filled with a porous medium saturated by a binary fluid for which the Soret effect is taken into account. Dirichlet and Neumann boundary conditions for temperature are applied to the horizontal walls ($z = 0$, $z = H$). The vertical walls ($x' = 0$, $x' = L$) are impermeable and adiabatic. All the boundaries are assumed rigid. The cavity is subjected to linear harmonic oscillations in the vertical direction (amplitude b and dimensional frequency ϖ). For the governing equations, we adopt the Boussinesq approximation and Darcy equation for which the non-stationary term is taken into account.

We set all the properties of the binary fluid constant except the density ρ in the buoyancy term, which depends linearly on the local temperature and mass fraction:

$$\rho = \rho_r[1 - \beta_T(T' - T_r) - \beta_C(C' - C_r)], \qquad (1)$$

where ρ_r is the fluid mixture density at temperature T_r and mass fraction C_r. β_T and β_C are the thermal and concentration expansion coefficients respectively.

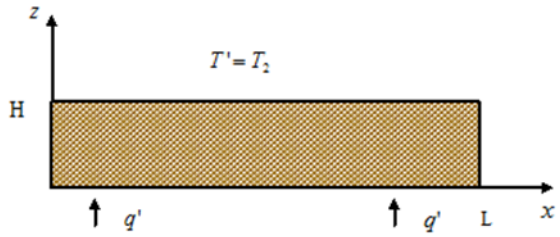

Fig. 1. A rectangular cavity, H is the height and L is the width, the low horizontal plate is submitted to constant uniform heat flux and the top one is maintained to a constant temperature while no mass flux is imposed

When we consider the referential related to the oscillating system, the gravitational field $\boldsymbol{g}$ is replaced by $\boldsymbol{g} + b\varpi^2 \sin(\varpi\, t')\, \boldsymbol{e}_z$ where $\boldsymbol{e}_z$ is the unit vector along the vertical axis (vibration axis) and t' the dimensional time.

The reference scales are H for the length, $\sigma H^2/a$ for the time, with $a = \lambda^*/(\rho c)_f$ and $\sigma = (\rho c)^*/(\rho c)_f$ (where λ^* and $(\rho c)^*$ are, respectively, the effective thermal conductivity and volumetric heat capacity of the porous medium), a/H for the velocity (a is the effective thermal diffusivity), $\Delta T = q'H/\lambda^*$ for the temperature and $\Delta C = -\Delta T\, C_i(1 - C_i)\, D_T^*/D^*$ for the mass fraction, where C_i, D_T^*, D^* are the initial mass fraction, the thermodiffusion and the mass diffusion coefficients of the denser component, respectively. The dimensionless temperature and mass fraction are, respectively, defined by $T = (T' - T_2)/\Delta T$, $C = (C' - C_i)/\Delta C$.

Thus, the dimensionless governing conservation equations for mass, momentum, energy and chemical species, where the Soret effect is taken into account, are

$$\begin{cases} \boldsymbol{\nabla} \cdot \boldsymbol{V} = 0, \\ B\partial_t \boldsymbol{V} + \boldsymbol{V} = -\boldsymbol{\nabla} P + Ra(T + \psi C)(1 - R\sin(\omega t))\, \boldsymbol{e}_z, \\ \partial_t T + \boldsymbol{V} \cdot \boldsymbol{\nabla} T = \nabla^2 T, \\ \epsilon \partial_t C + \boldsymbol{V} \cdot \boldsymbol{\nabla} C = \dfrac{1}{Le}(\nabla^2 C - \nabla^2 T), \end{cases} \qquad (2)$$

where $B = Da(\rho c)_f/(\rho c)^* \epsilon \Pr$ is the inverse Vadasz number ($B = 1/Va$), $Da = K/H^2$ is the Darcy number and K the permeability of the porous medium.

The problem under consideration depends on eight non-dimensional parameters: the thermal Rayleigh number, $Ra = Kg\beta_T H\Delta T/a\nu$, $R = b\omega'^2/g$, the separation ratio $\psi = -(\beta_c/\beta_T)\,(D_T/D)\, C_i(1 - C_i)$, the Lewis number $Le = a^*/D^*$, the normalized porosity $\epsilon = \epsilon^*(\rho c)_f/(\rho c)^*$ (where ϵ^* is the porosity), the dimensionless frequency $\omega = \omega'^2(\rho c)^* H^2/a^*(\rho c)_f$, the aspect ratio A and the factor B. The dimensionless boundary conditions are

$$\begin{cases} \boldsymbol{V} \cdot \boldsymbol{n} = 0, & \forall M \in \partial\Omega, \\ \dfrac{\partial C}{\partial z} = \dfrac{\partial T}{\partial z} = -1, & z = 0\ \forall x \in [0, A], \\ \dfrac{\partial C}{\partial z} = \dfrac{\partial T}{\partial z}, & z = 1\ \forall x \in [0, A], \\ T = 0, & z = 1\ \forall x \in [0, A], \\ \dfrac{\partial C}{\partial x} = \dfrac{\partial T}{\partial x} = 0, & x = 0, A\ \forall z \in [0, 1]. \end{cases} \qquad (3)$$

In the momentum equation the term $B\partial \boldsymbol{V}/\partial t$ is usually neglected since B is of order 10^{-6}. However, in our problem, high-frequency vibrations cause very large accelerations, making it necessary to consider this non-stationary term [6].

3 The averaged equations

In the limiting case of high-frequency and small-amplitude vibrations, the averaging method can be applied to study thermal vibrational convection. According to this method, each field ($\boldsymbol{V}$, P, T, C) is subdivided into two parts: the first part varies slowly with time (*i.e.*, the characteristic time is large with respect to the period of the vibrations) and the second one varies quickly with time (*i.e.*, the characteristic time is of the order of magnitude of the vibrational period):

$$(\boldsymbol{V}, P, T, C) = (\boldsymbol{V}^*, P^*, T^*, C^*)(t) + (\boldsymbol{u}', p', \theta', c')(\omega, t). \tag{4}$$

Here, $\boldsymbol{V}^*$, P^*, T^*, C^* are the averaged fields (*i.e.*, the mean value of the field calculated over the period $\tau = 2\pi/\omega$) of the velocity, pressure, temperature and mass fraction. The decoupling between the pulsational parts of the velocity and the pressure is obtained by using a Helmholtz decomposition:

$$(T^* + \psi C^*)\boldsymbol{e}_z = \boldsymbol{W} + \boldsymbol{\nabla}\xi, \tag{5}$$

where $\boldsymbol{W}$ is the solenoidal part of $(T^* + \psi C^*)\boldsymbol{e}_z$ satisfying $\boldsymbol{\nabla}\cdot\boldsymbol{W} = 0$. Thus, the averaged flow equations are

$$\begin{cases} \boldsymbol{\nabla}\cdot\boldsymbol{V}^* = 0, \\ B\partial_t \boldsymbol{V}^* + \boldsymbol{V}^* = -\boldsymbol{\nabla}P^* + (Ra(T^* + \Psi C^*) \\ +Rv\left(\boldsymbol{\nabla}T^* + \dfrac{\Psi}{\epsilon^*}\boldsymbol{\nabla}C^*\right)\cdot\boldsymbol{W})\boldsymbol{e}_z, \\ \partial_t T^* + (\boldsymbol{V}^*\cdot\boldsymbol{\nabla})T^* = \nabla^2 T^*, \\ \epsilon\partial_t C^* + (\boldsymbol{V}^*\cdot\boldsymbol{\nabla})C^* = \dfrac{1}{Le}(\nabla^2 C^* - \nabla^2 T^*), \\ (T^* + \psi \mathrm{C}^*)\boldsymbol{e}_z = \boldsymbol{W} + \boldsymbol{\nabla}\xi, \\ \boldsymbol{\nabla}\cdot\boldsymbol{W} = 0. \end{cases} \tag{6}$$

In addition to the boundary conditions (6)–(10) applied to the mean fields, we assume that

$$\boldsymbol{W}\cdot\boldsymbol{n} = 0 \quad \text{on } \partial\Omega. \tag{7}$$

The modified vibrational Rayleigh number $Rv = \frac{Ra^2R^2B}{2(B^2\omega^2+1)}$ characterizes the intensity of the vibrations.

4 Linear stability of the equilibrium solution in an infinite horizontal porous layer

The stability of the equilibrium solution was studied by Charrier-Mojtabi *et al.* [8]. They restricted their study to the case $Le = 2$ for which the fluid considered is in the gaseous state, and so the Dufour effect should be taken into account. We extended this study to the case of a high Lewis number and we focused on the transition from the equilibrium solution to the unicellular flow obtained for binary mixtures.

This problem admits a mechanical equilibrium solution characterized by

$$\boldsymbol{V}_0^* = \boldsymbol{0}, \quad T_0^* = -z + cst, \quad C_0^* = -z + \frac{1}{2}, \quad \boldsymbol{W}_0 = \boldsymbol{0}. \tag{8}$$

In order to analyze the stability of this conductive solution, we introduce the velocity stream function ψ', temperature θ, the transformation $\eta = c - \theta$, and finally, the solenoidal stream function φ', characterized by $v_x = \frac{\partial\psi'}{\partial z}$, $v_z = -\frac{\partial\psi'}{\partial x}$ and $w_x = \frac{\partial\varphi'}{\partial z}$, $w_z = -\frac{\partial\varphi'}{\partial x}$.

We assumed that the perturbations $(\widetilde{\psi}'(z), \widetilde{\theta}(z), \tilde{c}(z), \widetilde{\varphi}'(z))$ are small. The perturbation quantities are chosen as follows:

$$(\psi', \theta, c, \varphi') = \left(\widetilde{\psi}'(z), \widetilde{\theta}(z), \tilde{c}(z), \widetilde{\varphi}'(z)\right) e^{Ik_x x + \sigma t}. \tag{9}$$

We introduce a new function $\widetilde{\eta} = \widetilde{c} - \widetilde{\theta}$. The system of equations can be written as

$$\begin{cases} (B\sigma + 1)(D^2 - k^2)\widetilde{\psi}' + Raik((1+\psi)\widetilde{\theta} + \psi\widetilde{\eta}) \\ -Rv\widetilde{\varphi}'k^2\left(1 + \dfrac{\psi}{\epsilon}\right) = 0, \\ (D^2 - k^2)\widetilde{\theta} - \sigma\widetilde{\theta} - \mathrm{i}k\widetilde{\psi}' = 0, \\ (D^2 - k^2)\widetilde{\eta}/Le - \epsilon\sigma(\widetilde{\eta} + \widetilde{\theta}) - \mathrm{i}k\widetilde{\psi}' = 0, \\ (D^2 - k^2)\widetilde{\varphi}' + \mathrm{i}k((1+\psi)\widetilde{\theta} + \psi\widetilde{\eta}) = 0, \end{cases} \tag{10}$$

where $D = \frac{\partial}{\partial z}$, k is the wave number in the horizontal (ox) direction, $I^2 = -1$, and σ is the temporal exponential growth rate of perturbation. The corresponding boundary conditions are

$$\begin{cases} z = 0\text{: } \widetilde{\psi}' = \widetilde{\varphi}' = \dfrac{\partial\widetilde{\theta}}{\partial z} = \dfrac{\partial\widetilde{\eta}}{\partial z} = 0; \\ z = 1\text{: } \widetilde{\psi}' = \widetilde{\varphi}' = \widetilde{\theta} = \dfrac{\partial\widetilde{\eta}}{\partial z} = 0. \end{cases} \tag{11}$$

4.1 Limiting case of the long-wave mode instability

We study the special case of the long-wave mode theoretically. In some related studies in fluid media, Razi *et al.* [11] showed that the asymptotic analysis results in a closed form relation for the stability threshold. In order to obtain such a relation, a regular perturbation method with the wave number as the small parameter is performed (for simplifying the procedure), we drop the tilde symbol and we expand $(\psi', \theta, \eta, \varphi', \sigma)$ as

$$(\psi', \theta, \eta, \varphi', \sigma) = \sum_{n=0}^{\infty} k^n(\psi'_n, \theta_n, \eta_n, \varphi'_n, \sigma_n), \tag{12}$$

with boundaries conditions:

$$\begin{cases} z=0\text{: } \psi_n' = \varphi_n' = \dfrac{\partial \theta_n}{\partial z} = \dfrac{\partial \eta_n}{\partial z} = 0; \\ z=1\text{: } \psi_n' = \varphi_n' = \theta_n = \dfrac{\partial \eta_n}{\partial z} = 0. \end{cases} \tag{13}$$

By substituting expressions in the amplitude equations resulting from the linear stability analysis and factoring the same order of k, we find a sequential system of equations:

For the zeroth order (k^0):

$$\psi_0' = 0, \quad \varphi_0' = 0, \quad \theta_0 = 0, \quad \eta_0 = cst, \quad \sigma_0 = 0. \tag{14}$$

At order 1, we get:

$$\begin{cases} \theta_1 = 0, \quad \psi_1' = -IRa\psi\eta_0(z^2-z)/2, \quad \eta_1 = cst, \\ \varphi_1' = -I\psi\eta_0(z^2-z)/2, \qquad\qquad\quad \sigma_1 = 0 \end{cases} \tag{15}$$

and at order 2:

$$\begin{cases} \theta_2 = Ra\psi\eta_0(z^4-2z^3+1)/24, \\ \psi_2' = -IRa\psi\eta_1(z^2-z)/2, \\ \eta_2 = \dfrac{\eta_0 z^2}{2}(Le\epsilon\sigma_2+1) + \dfrac{RaLe\psi\eta_0}{24}z^3(z-2), \\ \varphi_2' = -I\psi\eta_1(z^2-z)/2. \end{cases} \tag{16}$$

After involving the solvability condition, we find:

$$\epsilon\sigma_2 = \frac{1}{Le} - \psi\frac{Ra}{12}\,. \tag{17}$$

We note that σ_2 is real indicating that the conductive solution loses stability through a stationary bifurcation. For the marginal stability σ_2 is set equal to zero and we obtain the Rayleigh number:

$$Ra = \frac{12}{\psi Le}\,. \tag{18}$$

4.2 Stability analysis results for arbitrary values of wave number

The disturbances are developed in terms of polynomial functions verifying all the boundary conditions except those along the inner plates:

$$\begin{cases} \psi' = \displaystyle\sum_{n=1}^{N} a_n(1-z)z^n, \\ \theta = b_1\left(z^2 - \dfrac{2}{3}z^3\right) + b_2\left(z^3-1\right) + \displaystyle\sum_{n=1}^{N} b_{n+2}(1-z)^2 z^{n+1}, \\ \eta = d_1 + d_2\left(z^2 - \dfrac{2}{3}z^3\right) + \displaystyle\sum_{n=1}^{N} d_{n+2}(1-z)^2 z^{n+1}, \\ \varphi' = \displaystyle\sum_{n=1}^{N} e_n(1-z)z^n. \end{cases} \tag{19}$$

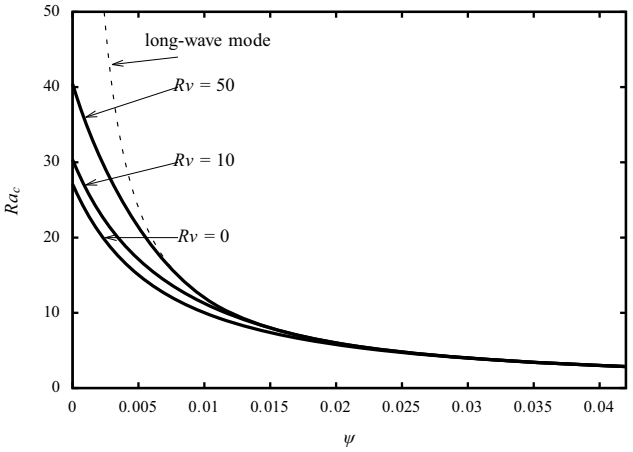

Fig. 2. Effect of vertical vibration on the onset of convection for $Le = 100$, $\epsilon = 0.5$ and $B = 10^{-6}$.

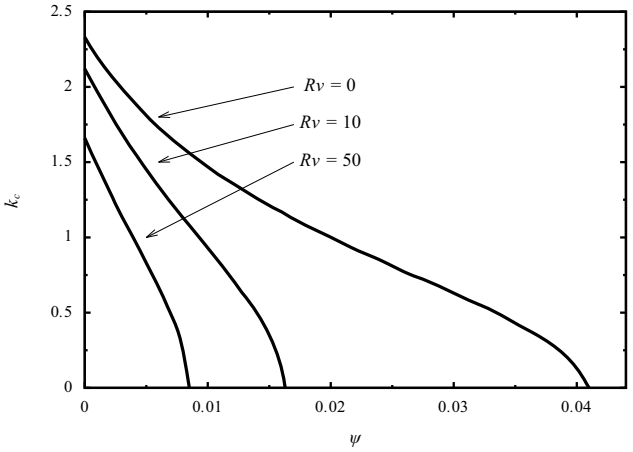

Fig. 3. Effect of vertical vibration on the critical wave number at the onset of convection for $Le = 100$, $\epsilon = 0.5$ and $B = 10^{-6}$.

The Tau spectral method used is similar to the Galerkin method. The test functions used for ψ', θ, φ' and η verify all the boundary conditions.

For $\psi > 0$ the first bifurcation is stationary. The results are presented in the stability diagram $Ra_c = f(\psi)$ and $kc = f(\psi)$. Figures 2 and 3 illustrate the effect of vibration on the onset of convection. For the case $Le = 100$, $\epsilon = 0.5$, $B = 10^{-6}$ and for $Rv = 0$, 10, 50, it can be noted that Ra_c increases with Rv whereas k_c decreases with Rv. Figure 4 shows the influence of vibrations on ψ_{uni}, the separation ration beyond which the critical wave number vanishes ($k_c = 0$), decreases. We note that ψ_{uni} decreases and becomes close to zero when Rv increases. So by adding vibrations, we can separate most binary mixtures. In the case $Rv = 0$, we obtain $\psi_{uni} = \frac{1}{\frac{10}{39}Le-1}$. Table 1 provides a comparison of the critical Rayleigh and wave numbers of the classical situation (absence of vibration) with the situation under different values of vibrational Rayleigh number.

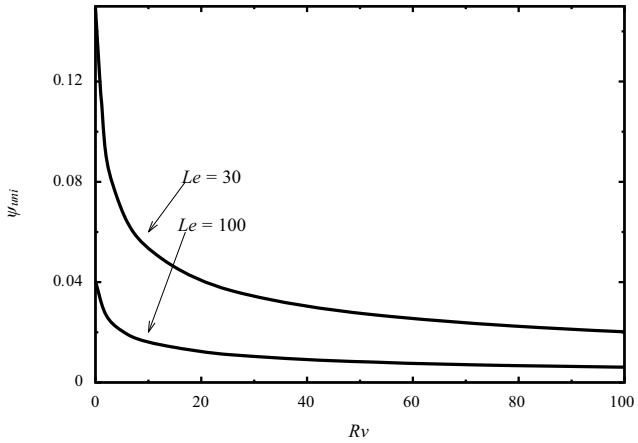

Fig. 4. Effect of the vertical vibration on the onset of the unicellular separation ratio beyond which the flow at the onset of convection becomes unicellular for $\epsilon = 0.5$ and $B = 10^{-6}$.

Table 1. Comparison of the critical Rayleigh and the wave number for $Le = 100$, $\epsilon = 0.5$ and $B = 10^{-6}$.

ψ	$Rv = 0$		$Rv = 10$		$Rv = 50$	
	Ra_c	k_c	Ra_c	k_c	Ra_c	k_c
0	27.10	2.33	30.35	2.12	40.43	1.66
0.001	23.56	2.20	26.55	1.97	35.29	1.48
0.002	20.75	2.09	23.49	1.83	30.98	1.31
0.004	16.59	1.90	18.88	1.57	24.16	0.99
0.005	15.03	1.81	17.11	1.45	21.41	0.83

5 Analytical solution of the unicellular flow

In the case of a shallow cavity ($A \gg 1$) in order to solve the problem analytically, the parallel flow approximation is considered [9, 12]. The streamlines are assumed to be parallel to the horizontal walls except for the vicinity of the vertical walls. In this case, the vertical component of velocity can be neglected. The temperature and mass fraction profiles are written as the sum of two terms: the first one defining the linear longitudinal variation and the second one giving the transverse distribution: The basic flow, denoted with a subscript 0, is then given as follows:

$$\begin{cases} \boldsymbol{V}_0 = U(z)\boldsymbol{e}_x, & T_0 = bx + h(z), \\ C_0 = mx + g(z), & \boldsymbol{W}_0 = W_1(z)\boldsymbol{e}_x, \end{cases} \tag{20}$$

where b and m are, respectively, the unknown constant temperature gradient and mass fraction gradient in the x-direction. For the stationary state, when the above-mentioned assumptions are made and the corresponding boundary conditions are considered, we obtain the velocity, temperature and concentration fields:

$$\begin{cases} U(z) = -\psi_0(2z-1), & W_1(z) = -\dfrac{\psi_0}{Ra}(2z-1), \\ T_0 = -z + 1, & C_0 = mx + g(z), \end{cases} \tag{21}$$

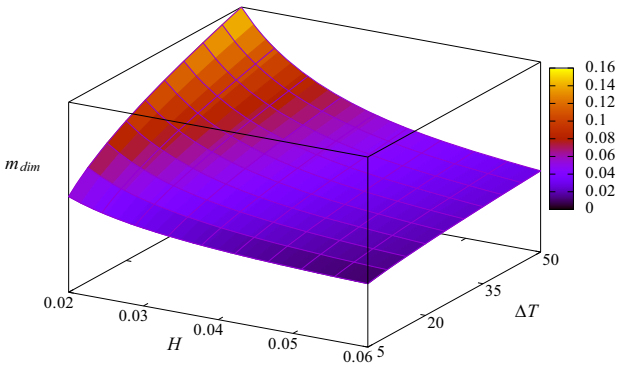

Fig. 5. Curve of dimensional mass fraction gradient m_{dim} for a mixed water ethanol (60.88% by weight of water), for ($\beta_c = 0.2$, $K = 10^{-9}$, $C_0 = 0.5$, $D = 4 \cdot 10^{-10}$, $D_T = 10^{-12}$, $\nu = 3 \cdot 10^{-6}$).

with

$$\begin{cases} \psi_0 = \dfrac{1}{2} Ra\psi m, \\ g(z) = \dfrac{\psi_0 m Le(6z^2 - 4z^3 - 1)}{12} + \dfrac{1 - mA}{2} - z, \\ m = \dfrac{5Le\psi_0}{Le^2\psi_0^2 + 30}. \end{cases} \tag{22}$$

Then we have $2{\psi_0}^3 Le^2 + (60 - 5RaLe\psi)\psi_0 = 0$ whose solutions are $\psi_0 = 0$ *and* $\psi_0 = \pm\frac{1}{2}\frac{\sqrt{10RaLe\psi - 120}}{Le}$.

The dimensionless and the dimensional mass fraction gradient are

$$m = \pm\frac{\sqrt{10RaLe\psi - 120}}{RaLe\psi}, \quad m_{dim} = \frac{\sqrt{10q_1q_2H\Delta T - 120}}{H^2 q_1}, \tag{23}$$

where $q_1 = Kg\beta_c/\nu D$ and $q_2 = -C_0(1 - C_0)D_T/D$.

Figure 5 illustrates the evaluation of the dimensional mass fraction gradient m_{dim} according to H and ΔT for a mixed water ethanol (60.88% by weight of water). It follows that for a fixed height of the cavity H, the mass fraction gradient will be so much greater than ΔT is great, while the H that maximizes the mass fraction gradient depends on the choice of ΔT, which is equal to $H_{max} = \frac{16}{q_1 q_2 \Delta T}$.

6 Linear stability analysis of the unicellular flow

In order to analyse the stability of the unicellular flow, we introduce the perturbation of the vertical velocity component $\boldsymbol{w}$, the perturbation of the vertical component of $\boldsymbol{W}$, $\boldsymbol{w}_2$, the perturbation of temperature θ, the concentration c and the transformation $\eta = c - \theta$. The disturbances are developed in the form of normal modes. It is assumed that the perturbation quantities are sufficiently small so that the second-order terms may be neglected. The system of

equations for the amplitudes can be written as

$$\begin{cases} (B\sigma+1)(D^2-k^2)w + Rak^2[(1+\psi)\theta+\psi\eta] \\ +Rv\left[IkDw_2\left(b+\frac{\psi}{\epsilon}m\right)\right. \\ \left.+k^2w_2\left(DT_0+\frac{\psi}{\epsilon}DC_0\right)+Ik^3w_2[(1+\psi)\theta+\psi\eta]\right]=0, \\ Ik(D^2-k^2)\theta-\sigma Ik\theta-wIkDT_0+Uk^2\theta+bDw=0, \\ \frac{Ik}{Le}(D^2-k^2)(\eta+\theta)-\sigma Ik(\eta+\theta)-wIkDC_0 \\ +Uk^2(\eta+\theta)+mDw=0, \\ (D^2-k^2)w_2+k^2[(1+\psi)\theta+\psi\eta]=0. \end{cases} \tag{24}$$

The corresponding boundary conditions are given as

$$\begin{cases} w=0, \quad \theta=\dfrac{\partial\eta}{\partial z}=0, \quad w_2=0 \qquad \text{for } z=1, \\ w=0, \quad \dfrac{\partial\theta}{\partial z}=\dfrac{\partial\eta}{\partial z}=0, \quad w_2=0 \quad \text{for } z=0. \end{cases} \tag{25}$$

The linear stability equations were solved using the 4th-order Galerkin method:

$$\begin{cases} w=\displaystyle\sum_{n=1}^{N} a_n(1-z)z^n, \\ \theta= b_1\left(z^2-1\right)+b_2\left(z^3-1\right)+\displaystyle\sum_{n=1}^{N} b_{n+2}\left(z^2-1\right)z^{n+1}, \\ \eta=d_1+d_2\left(z^2-\dfrac{2}{3}z^3\right)+\displaystyle\sum_{n=1}^{N} d_{n+2}(1-z)^2z^{n+1}, \\ w_2=\displaystyle\sum_{n=1}^{N} e_n(1-z)z^n. \end{cases} \tag{26}$$

For the value of ψ and Le studied, the critical Rayleigh number leading to stationary bifurcation is always higher than the one leading to Hopf bifurcation. So, in this study we focus on the critical number related to the Hopf bifurcation. The results are illustrated in table 2 for the case $\psi = 0.3$, $Le = 100$, $\epsilon = 0.5$, $A = 10$ and $B = 10^{-6}$, the vertical vibrations have a stabilizing effect on convective motions and increase the value of the critical thermal Rayleigh number Ra_c. Thus the vibrations can be used to maintain the unicellular flow and allow species separation over a wider range of Rayleigh numbers. It should be mentioned that vibrations reduce the critical wave numbers k_c and the Hopf frequency ω_c. This means that vibrations can also be used to decrease the number of convective cells at the transition from the unicellular flow to the multicellular flow.

Table 2. Effect of vibrations on the critical values of the Rayleigh number Ra_c, wave number k_c and frequency ω_c associated with the transition from unicellular to multicellular flow for $\psi = 0.3$, $Le = 100$, $\epsilon = 0.5$ and $B = 10^{-6}$.

Rv	k_c	Ra_c	ω_c
0	5.25	16.87	1.55
10	4.98	17.09	1.44
30	4.54	17.39	1.27
50	4.20	17.55	1.14
70	3.94	17.59	1.04

7 2D Numerical simulations

The averaged equations (eq. (6)) with the associated boundary conditions were solved using the finite element method. The influence of vibrations on the onset of convection was investigated for a cell of aspect ratio $A = 10$ for $Le = 100$ and $\epsilon = 0.5$ (B is fixed to 10^{-6}). It was observed that the critical parameters of the bifurcations differed very little between the case $A = 10$ and the case of a cell of infinite horizontal extention. A structured mesh 150×30 was used for the finite element method for $A = 10$. For the onset of stationary convection, the results for $Le = 100$ are presented in figs. 6 and 7. For $\psi = 0.02$, without vibration ($Rv = 0$), the critical parameters $Ra_c = 5.78$, $k_c = 1.00$ are obtained from the linear stability analysis. For the same value of ψ but with vibrations ($Rv = 10$), we obtain $Ra_c = 6$, $k_c = 0$ from the linear stability analysis, so the critical wave numbers is zero, which means that the flow at the onset of convection is unicellular. To confirm this result, we used the direct numerical simulation to study the case $\psi = 0.02$ for a value of Ra close to the critical value ($Ra = 6$) first without vibrations ($Rv = 0$) and then with vibrations ($Rv = 10$).

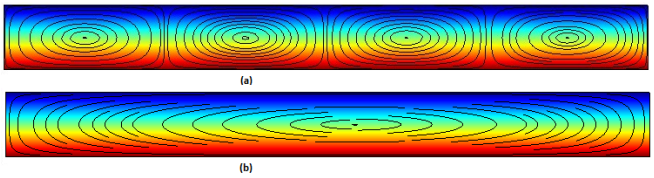

Fig. 6. Streamlines for $Le = 100$, $\psi = 0.02$, $Ra = 6$. (a) $Rv = 0$ (without vibration); (b) $Rv = 10$. A multicellular flow is obtained at the transition from the equilibrium solution for $Rv = 0$, whereas a unicellular flow is obtained for $Rv = 10$.

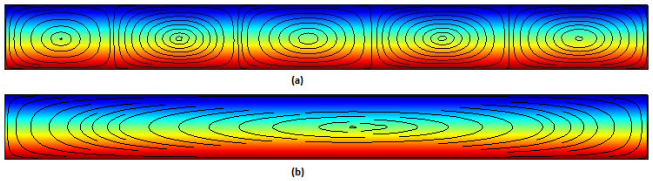

Fig. 7. Streamlines for $Le = 100$, $\psi = 0.01$, $Ra = 12.2$. (a) $Rv = 10$ (without vibration); (b) $Rv = 50$. A multicellular flow is obtained at the transition from the equilibrium solution for $Rv = 10$, whereas a unicellular flow is obtained for $Rv = 50$.

Figure 6(a) shows the streamlines for $Rv = 0$. In this case, the flow is multicellular and we cannot use the horizontal cell to separate the components of a binary mixture. Figure 6(b) shows the streamlines for the same values of all the parameters but with vibrations. It can be observed that vibrations modify the structure of the flow from multicellular to unicellular. Similar results were obtained for $\psi = 0.01$ (fig. 7).

8 Conclusions

The two-dimensional thermosolutal Soret-driven convection under mechanical vibration was studied analytically and numerically. The vibration was in the limiting range of high frequency and small amplitude and its direction was taken parallel to the temperature gradient. The geometries considered were an infinite horizontal layer and a confined cavity. The linear stability analysis of equilibrium and unicellular solutions were studied for the positive value of ψ. The equilibrium solution was found to lose its stability via a stationary bifurcation. For the long-wave mode, the Rayleigh number was obtained as $Ra = \frac{12}{Le\psi}$. It was observed that the vertical vibrations have a stabilizing effect on convection. The vibrations could be used to decrease the value of the separation factor leading to the unicellular flow ψ_{uni}, allowing separation in the binary mixture in a horizontal cell for a broad range of binary mixtures. The dimensional mass fraction gradient m_{dim} was defined according to H and ΔT. It followed that, for a fixed height of the cavity H, the mass fraction gradient increases with ΔT, while the height that maximizes the mass fraction gradient is $H_{max} = \frac{16}{q_1 q_2 \Delta T}$. The expression of the analytical relation is $S = A \cdot \frac{\sqrt{10RaLe\psi - 120}}{RaLe\psi}$ giving that the separation value is identical to the one obtained by Elhajjar *et al.* [9] for a cell with horizontal walls maintained at constant but different temperatures.

This research is supported by the CNES (Centre National d'Études Spatiales).

Author contribution statement

AA and AM conceived of the presented idea and supervised the findings of this work. SO and AM developed the theory and performed the computations. AA and AM verified the analytical methods and encouraged SO to compare numerical simulations and analytical results. All authors discussed the results and contributed to the final manuscript.

References

1. D.A. Nield, A. Bejan, *Convection in Porous Media*, 4th edition (Springer Inc., New York, 2013).
2. H. Khallouf, G.Z. Gershuni, A. Mojtabi, Numer. Heat Transfer, Part A: Appl. **30**, 605 (1996).
3. G.Z. Gershuni, A.K. Kolesnikov, J.C. Legros, B.I. Myznikova, J. Fluid Mech. **330**, 251 (1997).
4. G.Z. Gershuni, D.V. Lyubimov, *Thermal Vibrational Convection* (John Wiley and Sons, 1998) p. 358.
5. G.Z. Gershuni, A.K. Kolesnikov, J.C. Legros, B.I. Myznikova, Int. J. Heat Mass Transfer **42**, 547 (1999).
6. S.M. Zen'kovskaya, T.N. Rogovenko, J. Appl. Mech. Tech. Phys. **40**, 379 (1999).
7. G. Bardan, A. Mojtabi, Phys. Fluids **12**, 1 (2000).
8. M.C. Charrier-Mojtabi, Y.P. Razi, K. Maliwan, A. Mojtabi, Numer. Heat Transfer, Part A: Appl. **46**, 981 (2004).
9. B. Elhajjar, A. Mojtabi, M.C. Charrier-Mojtabi, Int. J. Heat Mass Transfer **52**, 165 (2009).
10. D. Lyubimov, E. Kolchanova, T. Lyubimova, Transp. Porous Media **106**, 237 (2015).
11. Y.P. Razi, M.C. Charrier-Mojtabi, A. Mojtabi, Transp. Porous Media **22**, 149 (2008).
12. R. Bennacer, A. Mahidjiba, P. Vasseur, H. Beji, R. Duval, Int. J. Numer. Methods Heat Fluid Flow **13**, 199 (2003).